Signal Temporal Logic-Guided Apprenticeship Learning *Supplemental Document*

Aniruddh G. Puranic, Jyotirmoy V. Deshmukh and Stefanos Nikolaidis

***Abstract*—In this document, we cover the quantitative semantics of Signal Temporal Logic (STL) in Appendix A, theory related to affine transformations in rewards in Appendix B, and all details of experiments in Appendix C.**

Appendix A
Signal Temporal Logic

Definition A.1 (Quantitative Semantics for Signal Temporal Logic)**.** Given an algebraic structure $(\oplus, \otimes, \top, \bot)$, we define the quantitative semantics for an arbitrary signal $\mathbf{x}$ against an STL formula φ at time t as in Table I.

TABLE I
Quantitative Semantics of STL

φ	$\rho(\varphi, \mathbf{x}, t)$
$true/false$	$\top/\bot$
μ	$f(\mathbf{x}(t))$
$\neg\varphi$	$-\rho(\varphi, \mathbf{x}, t)$
$\varphi_1 \wedge \varphi_2$	$\otimes(\rho(\varphi_1, \mathbf{x}, t), \rho(\varphi_2, \mathbf{x}, t))$
$\varphi_1 \vee \varphi_2$	$\oplus(\rho(\varphi_1, \mathbf{x}, t), \rho(\varphi_2, \mathbf{x}, t))$
$\mathbf{G}_I(\varphi)$	$\otimes_{\tau \in t+I}(\rho(\varphi, \mathbf{x}, \tau))$
$\mathbf{F}_I(\varphi)$	$\oplus_{\tau \in t+I}(\rho(\varphi, \mathbf{x}, \tau))$
$\varphi \mathbf{U}_I \psi$	$\oplus_{\tau_1 \in t+I}(\otimes(\rho(\psi, \mathbf{x}, \tau_1), \otimes_{\tau_2 \in [t, \tau_1)}(\rho(\varphi, \mathbf{x}, \tau_2)))$

A signal satisfies an STL formula φ if it is satisfied at time $t = 0$. Intuitively, the quantitative semantics of STL represent the numerical distance of "how far" a signal is away from the signal predicate. For a given requirement φ, a demonstration or policy d that satisfies it is represented as $d \models \varphi$ and one that does not, is represented as $d \not\models \varphi$. In addition to the Boolean satisfaction semantics for STL, various researchers have proposed quantitative semantics for STL, [1], [2] that compute the degree of satisfaction (or *robust satisfaction values*) of STL properties by traces generated by a system. In this work, we use the following interpretations of the STL quantitative semantics: $\top = +\infty$, $\bot = -\infty$, and $\oplus = \max$, and $\otimes = \min$, as per the original definitions of robust satisfaction proposed in [1], [3].

Appendix B
Derivations and Proofs

As mentioned in the main letter, we show that applying affine transformations to the reward function do not change the optimal policy. Particularly, we are concerned with scaling and shifting the rewards by a constant factor.

Lemma B.1. *The optimal policy is invariant to affine transformations in the reward function.*

Proof Sketch. From [4], we have the definition of the Q function as follows, for the untransformed reward function R:

$$Q(s,a) \doteq \mathbb{E}\left[\sum_{k=0}^{\infty} \gamma^k \cdot R(s,a)_{t+k+1} | S_t = s, A_t = a\right] \quad (1)$$

$$Q(s,a) \doteq R(s,a) + \gamma \sum_{s'} P(s,a,s') \max_{a'} Q(s',a') \quad (2)$$

We consider two cases of reward function affine transformations in our work: (a) scaling by a positive constant and (b) shifting by a constant. In both these cases, our objective is to express the new Q function in terms of the original. Note that we abbreviate $R(s,a)$ to just R for simplicity.

Case (a): Scaling R by a positive constant: Let the scaled reward function be defined as $R' = c \cdot R, c > 0$. The new Q function is then

$$Q'(s,a) \doteq \mathbb{E}\left[\sum_{k=0}^{\infty} \gamma^k \cdot R'_{t+k+1} | S_t = s, A_t = a\right]$$
$$Q'(s,a) = \mathbb{E}\left[\sum_{k=0}^{\infty} \gamma^k \cdot c \cdot R_{t+k+1} | S_t = s, A_t = a\right]$$
$$Q'(s,a) = c \cdot \mathbb{E}\left[\sum_{k=0}^{\infty} \gamma^k \cdot R_{t+k+1} | S_t = s, A_t = a\right]$$
$$Q'(s,a) = c \cdot Q(s,a)$$

Thus we see that the new Q function scales with the scaling constant.

From Equation 2 and by later substituting for Q' from the above result, we have,

$$Q'(s,a) \doteq R'(s,a) + \gamma \sum_{s'} P(s,a,s') \max_{a'} Q'(s',a')$$
$$c \cdot Q(s,a) = c \cdot R(s,a) + \gamma \sum_{s'} P(s,a,s') \max_{a'} (c \cdot Q(s',a'))$$
$$c \cdot Q(s,a) = c \cdot R(s,a) + c\gamma \sum_{s'} P(s,a,s') \max_{a'} \cdot Q(s',a')$$
$$Q(s,a) = R(s,a) + \gamma \sum_{s'} P(s,a,s') \max_{a'} \cdot Q(s',a')$$

Thus the Bellman equation holds indicating that the policy is invariant to scaling by a positive constant.

The authors are with the Department of Computer Science, University of Southern California, USA. Email: {puranic, jdeshmuk, nikolaid}@usc.edu

Case (b): Shifting R by a constant: Let the shifted reward function be defined as $R' = R + c$. The new Q function is then

$$Q'(s,a) \doteq \mathbb{E}\left[\sum_{k=0}^{\infty} \gamma^k \cdot R'_{t+k+1} | S_t = s, A_t = a\right]$$
$$Q'(s,a) = \mathbb{E}\left[\sum_{k=0}^{\infty} \gamma^k \cdot (R_{t+k+1} + c) | S_t = s, A_t = a\right]$$
$$Q'(s,a) = \mathbb{E}\left[\sum_{k=0}^{\infty} \gamma^k \cdot R_{t+k+1} | S_t = s, A_t = a\right] + \sum_{k=0}^{\infty} \gamma^k c$$
$$Q'(s,a) = Q(s,a) + \frac{c}{1-\gamma}$$

Thus we see that the new Q values get shifted by the constant.

From Equation 2 and by later substituting for Q' from the above result, we have,

$$Q'(s,a) \doteq R'(s,a) + \gamma \sum_{s'} P(s,a,s') \max_{a'} Q'(s',a')$$
$$Q(s,a) + \frac{c}{1-\gamma} = R(s,a) + c + \gamma \sum_{s'} P(s,a,s') \max_{a'} \left(Q(s',a') + \frac{c}{1-\gamma}\right)$$
$$Q(s,a) + \frac{c}{1-\gamma} = R(s,a) + c + \gamma \sum_{s'} P(s,a,s') \max_{a'} Q(s',a') + \gamma \sum_{s'} P(s,a,s') \frac{c}{1-\gamma}$$
$$Q(s,a) + \frac{c}{1-\gamma} = R(s,a) + \gamma \sum_{s'} P(s,a,s') \max_{a'} Q(s',a') + c + \frac{c\gamma}{1-\gamma}$$
$$Q(s,a) = R(s,a) + \gamma \sum_{s'} P(s,a,s') \max_{a'} \cdot Q(s',a')$$

Thus the Bellman equation holds indicating that the policy is invariant to shifting by a constant.

□

Therefore, any combination of scaling or shifting does not affect the optimal policy in our work. Similarly, the optimal policy is shown to be invariant towards reward shaping with potential functions [5].

APPENDIX C
EXPERIMENT DETAILS

This section describes additional details about the experiments such as the STL task specifications, hyperparameters, training and evaluation results.

A. Task - Discrete-Space Frozenlake

We make use of the $Frozenlake$ (FL) deterministic environments from OpenAI Gym [6] that consist of a grid-world of sizes 4x4 or 8x8 with a reach-avoid task. Informally, the task specifications are (i) eventually reaching the goal, (ii) always avoid unsafe regions and (iii) take as few steps as possible. In these small environments $m = 5$ demonstrations of varying optimality are manually generated. We use A2C as the RL agent and show the training results in Fig. 1. The left figures show the statistics of the rollout PGAs and the evolution of weights over time. The right figures show the rewards accumulated and episode lengths.

We see from the left figures, that initially, the non-uniform weights of specifications correspond to the suboptimal demonstrations. And over time, the weights all converge to $1/3$ indicating that there are no edges in the final DAG, while the PGAs of rollouts from the final policy are maximum, as hypothesized. Since the environments are deterministic, the final policy achieve a 100% success rate. Since the task can be achieved even with IRL-based methods, we compare the amount of demonstrations required. Under identical conditions, the minimum number of demonstrations used by MCE-IRL are 50 for 4x4 grid and 300 for 8x8 grid. The algorithm in [7] uses over 1000 demonstrations in the 8x8 grid, even though they use temporal logic specifications similar to ours. *This clearly suggests that the choice of the reward inference algorithm plays a significant role in sample complexity*. This is due to the unsafe regions being scattered over the map, requiring the desirable *dense* features to appear very frequently.

B. Task - Reaching Pose

The hyperparameters for both tasks: Panda-Reach and Needle-Reach, were nearly identical(Table II). The specifications for both these tasks are:

1) Reaching the target pose: $\varphi_1 := \mathbf{F}(\|ee_{pose} - target_{pose}\| \leq \delta)$, where ee indicates the end-effector and δ is the threshold used to determine success. For Panda-Reach, $\delta = 0.2$ and for Needle-Reach, $\delta = 0.025$.
2) Reaching the target as quickly as possible: $\varphi_2 := \mathbf{G}(t <= 50)$, where t is the time when the end-effector reaches the target.

TABLE II
REACH TASK HYPERPARAMETERS.

Parameters	Values: Panda-Reach	Values: Needle-Reach
# Demos	5	
Reward Model	Neural Network [200 → 200]	
RL		
Model	SAC+HER	
Training Timesteps	$2 \cdot 10^5$	$2.5 \cdot 10^5$
# AL-STL Cycles	5	5
Policy Network	Shared [64 → 64]	
Learning Rate	$3 \cdot 10^-4$	
Discount Factor γ	0.95	
Learning Starts	100	
Batch Size	256	
Polyak Update τ	0.005	
PGA λ	0.9	
Training Success Rate	100%	
Test Success Rate	100%	

C. Task - Placing Cube

The hyperparameters are given in Table III. The specifications for both these tasks are:

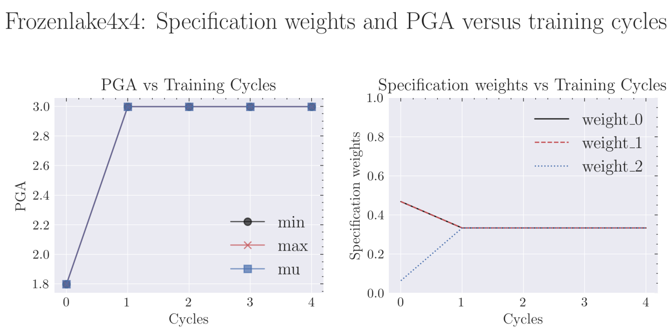

(a) FL4x4 Weights

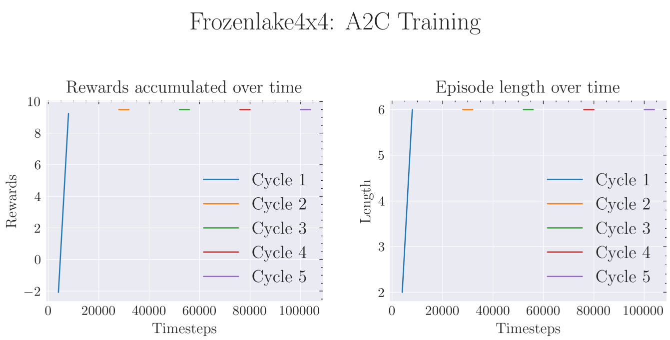

(b) FL4x4 Training Summary

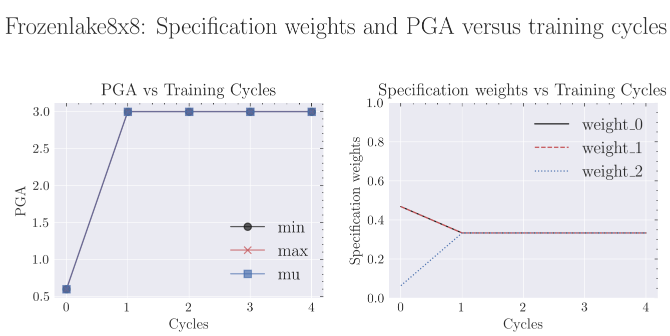

(c) FL8x8 Weights

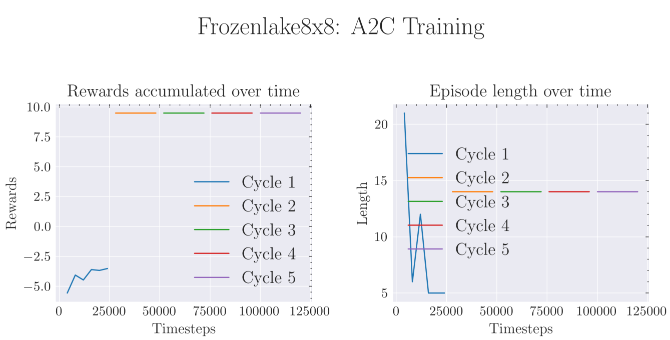

(d) FL8x8 Training Summary

Fig. 1. Results for the 4x4 and 8x8 Frozenlake environments.

1) Placing the cube at the target pose: $\varphi_1 := \mathbf{F}(\|cube_{pose} - target_{pose}\| \leq 0.05)$.
2) Reaching the target as quickly as possible: $\varphi_2 := \mathbf{G}(t <= 50)$, where t is the time when the end-effector reaches the target.

The statistics of the PGA shows that is maximum value is ≈ 6 since there are 2 specifications, each scaled by a factor of 3.

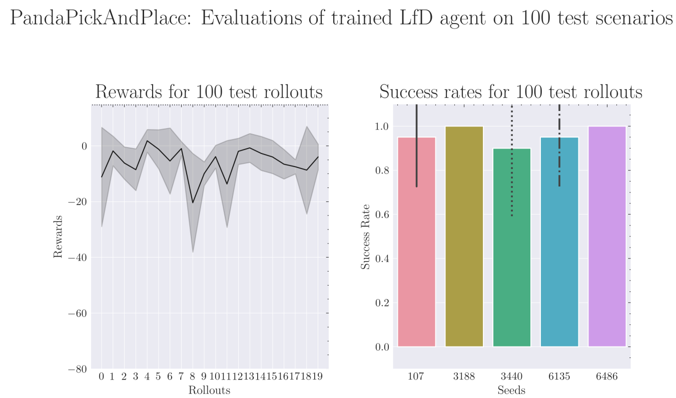

(a) Success rates on test trials

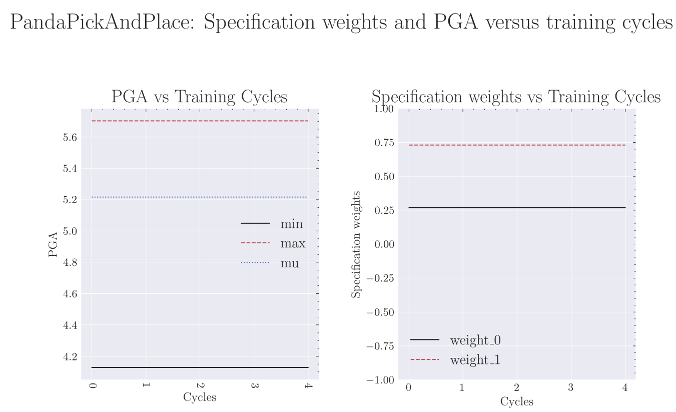

(b) PGA and Weights

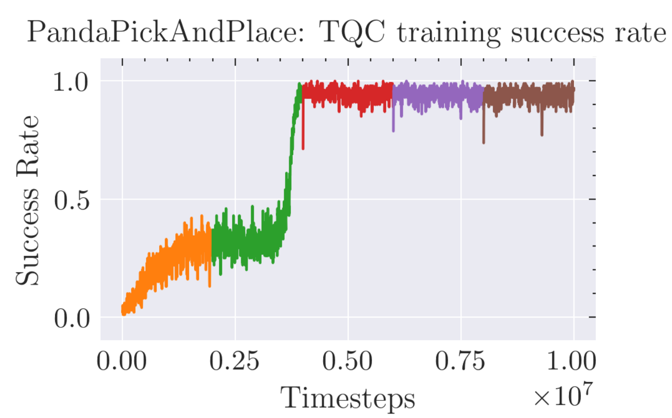

(c) RL training summary

Fig. 2. Summary of training and evaluations for the Cube-Placing task.

D. Task - Opening Door

The Panda robot uses operational space control to control the pose of the end-effector. The horizon for this task is 500

TABLE III
HYPERPARAMETERS FOR CUBE-PLACING TASK.

Parameters	Value
# Demos	5
Reward Model	Gaussian Process (Scale+RBF kernels)
RL	
Model	TQC+HER
Training Timesteps	10^7
# AL-STL Cycles	5
Policy Network	Shared $[512 \rightarrow 512 \rightarrow 512]$
Learning Rate	$1 \cdot 10^{-3}$
Discount Factor γ	0.95
Learning Starts	1000
Batch Size	2048
Polyak Update τ	0.05
PGA λ	0.9
Training Success Rate	98%
Test Success Rate	96%
Training Time	10.75 hours (2.15 hours/cycle)

and the control frequency is 20 Hz. The hyperparameters are given in Table IV. The specifications for both these tasks are:

1) Opening the door: $\varphi_1 := \mathbf{F}(\angle door\_hinge \geq 0.3)$. Angle is measured in radians.
2) Reaching the door handle: $\varphi_2 := \mathbf{F}(\|ee - door\_handle\| < 0.2)$; end-effector should be within $2cm$ of the door handle.

TABLE IV
HYPERPARAMETERS FOR DOOR-OPENING TASK.

Parameters	Value
# Demos	5
Reward Model	Neural Network $[16 \rightarrow 16 \rightarrow 16]$
RL	
Model	TQC
Training Timesteps	$5 \cdot 10^6$
# AL-STL Cycles	25
Policy Network	Shared $[256 \rightarrow 256]$
Learning Rate	$1 \cdot 10^{-3}$
Discount Factor γ	0.97
Learning Starts	100
Batch Size	256
Polyak Update τ	0.5
PGA λ	0.3
Training Success Rate	98%
Test Success Rate	100%
Training Time	6.5 hours (0.26 hours/cycle)

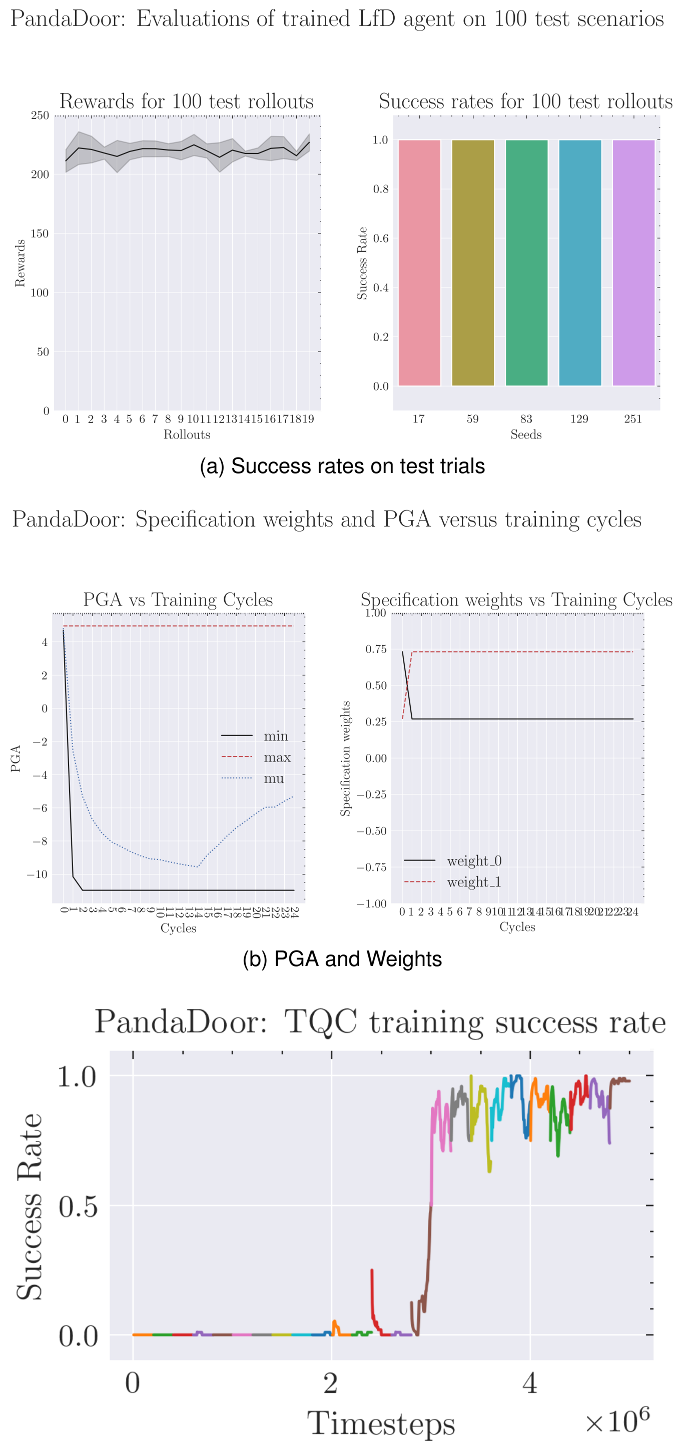

(a) Success rates on test trials

(b) PGA and Weights

(c) RL training summary

Fig. 3. Summary of training and evaluations for the Door-Opening task.

REFERENCES

[1] G. E. Fainekos and G. J. Pappas, "Robustness of temporal logic specifications for continuous-time signals," *Theoretical Computer Science*, 2009.

[2] S. Jaksic, E. Bartocci, R. Grosu, T. Nguyen, and D. Nickovic, "Quantitative monitoring of STL with edit distance," *Formal Methods in System Design*, 2018.

[3] A. Donzé and O. Maler, "Robust satisfaction of temporal logic over real-valued signals," in *FORMATS*, 2010.

[4] R. S. Sutton and A. G. Barto, *Reinforcement Learning: An Introduction*, 2nd ed. The MIT Press, 2018.

[5] A. Y. Ng, D. Harada, and S. Russell, "Policy invariance under reward transformations: Theory and application to reward shaping," in *ICML*. Morgan Kaufmann, 1999, pp. 278–287.

[6] G. Brockman, V. Cheung, L. Pettersson, J. Schneider, J. Schulman, J. Tang, and W. Zaremba, "Openai gym," *CoRR*, vol. abs/1606.01540, 2016.

[7] W. Zhou and W. Li, "Safety-aware apprenticeship learning," in *CAV*. Springer, 2018.